(14) D. W. Griffiths and M. L. Bender, *Adv. Catal.*, **23** 209 (1973).
(15) W. B. Gruhn and M. L. Bender, *Bioorg. Chem.*, **3**, 324 (1974).
(16) P. C. Manor and W. Saenger, *J. Am. Chem. Soc.*, **96**, 3630 (1974), and references therein.
(17) A. Wishnia and S. J. Lappi, *J. Mol. Biol.*, **82**, 77 (1974).
(18) K. Sensse and F. Cramer, *Chem. Ber.*, **102**, 509 (1969).
(19) M. Otagiri, K. Ikeda, K. Uekama, O. Ito, and M. Hatano, *Chem. Lett.*, 679 (1974).
(20) K. Flohr, R. M. Paton, and E. T. Kaiser, *J. Am. Chem. Soc.*, **97**, 1209 (1975).
(21) J. P. Kintzinger, J. M. Lehn, and R. L. Williams, *Mol. Phys.*, **17**, 135 (1969).
(22) C. Brevard, J. P. Kintzinger, and J. M. Lehn, *Tetrahedron*, **28**, 2429 (1972).
(23) R. Freeman and H. D. W. Hill, *J. Chem. Phys.*, **53**, 4103 (1970).
(24) R. Breslow and P. Campbell, *Bioorg. Chem.*, **1**, 140 (1971).
(25) G. C. Levy, J. D. Cargioli, and F. A. L. Anet, *J. Am. Chem. Soc.*, **95**, 1527 (1973).
(26) J. E. Anderson and P. A. Fryer, *J. Chem. Phys.*, **50**, 3784 (1969).
(27) C. Brevard and J. M. Lehn, *J. Am. Chem. Soc.*, **92**, 4987 (1970).
(28) C. Brevard, J. P. Kintzinger, and J. M. Lehn, *Tetrahedron*, **28**, 2447 (1972).
(29) M. D. Zeidler, *Ber. Bunsenges. Phys. Chem.*, **69**, 659 (1965).
(30) J. P. Behr and J. M. Lehn, *J. Chem. Soc., Perkin Trans. 2*, 1488 (1972).
(31) A. Hybl, R. E. Hundle, and D. E. Williams, *J. Am. Chem. Soc.*, **87**, 2779 (1965).
(32) B. D. Sykes, P. G. Schmidt, and G. R. Stark, *J. Biol. Chem.*, **245**, 1180 (1970).
(33) G. Navon and A. Lanir, *J. Magn. Reson.*, **8**, 144 (1972).
(34) P. Colson, H. J. Jennings, and I. C. P. Smith, *J. Am. Chem. Soc.*, **96**, 8081 (1974).
(35) E. F. Caldin, J. E. Crooks, D. O'Donnell, D. Smith, and S. Toner, *J. Chem. Soc., Faraday Trans. 1*, **68**, 849 (1972).
(36) J. Emert and R. Breslow, *J. Am. Chem. Soc.*, **97**, 670 (1975).

Metal–Metal Interactions Involving Metalloporphyrins. III. Conversion of Tetraphenylporphinatoiron(III) Azide to an N-Bridged Hemin Dimer[1]

David A. Summerville and Irwin A. Cohen*[2]

Contribution from the Departments of Chemistry, Polytechnic Institute of New York, Brooklyn, New York 11201, and Brooklyn College of the City University of New York, Brooklyn, New York 11210.

Received May 16, 1975

Abstract: The high temperature solution decomposition of tetraphenylporphinatoiron(III) azide ($TPPFe^{III}N_3$) in the absence of added base and oxygen has been examined. In addition to N_2 the only reaction product observed is formulated as TPPFeNFeTPP analogous to $(TPPFe)_2O$. The room temperature Mössbauer spectrum is sharp ($\delta = 0.10$, rel Fe; $\Delta = 1.08$ mm/s) and is compared to that of $(TPPFe)_2O$. Magnetic studies reveal a temperature independent moment indicative of one unpaired electron per dimer. The FeNFe infrared mode is observed at 910 (vs) and 885 (m) cm^{-1}. Kinetic studies of the solution thermolysis indicate first-order decomposition of $TPPFeN_3$ with $E_a = 33.7$ kcal/mol. This appears to be the first example of a nitrogen atom bridge between two metals of the first transition series.

Ever since the preparation of dinitrogen complexes of ruthenium(II)[3] the decomposition of coordinated azide has been of interest. Basolo and co-workers have been able to characterize the decomposition of Ru(III)[4] and Ir(III)[5] azides as proceeding through a strongly electrophilic protonated nitrene (e.g., $[(H_3N)_5Ru^{III}NH]^{3+}$ or $[(H_3N)_5Ir^{III}NH]^{3+}$). The fate of the intermediate depends in part on the available oxidation states of the metal ion. In the case of the ruthenium(II) catalyzed decomposition of azide[6] the corresponding intermediate has been proposed as $[(H_3N)_5Ru^{II}NH]^{2+}$ Because of the apparent nucleophicity of that intermediate Basolo and co-workers have pointed out that a $Ru^{II}\underset{\cdot\cdot}{\ddot{N}}H$ (nitrene) may be better represented as a $Ru^{IV}\ddot{N}H$ (protonated nitride or imido) species.

The only reported decomposition of a hemin azide was by McCoy and Caughey.[7] They observed that the infrared spectrum in the 2000-cm^{-1} region of azido protoporphyrin diethyl ester iron(III) in pyridine underwent a slow change at room temperature which was not inconsistent with the formation of a porphyrin $Fe^{II}N_2$ species. The spectral changes were not observed in the absence of pyridine or with other porphyrins. Because that product has not been fully characterized we investigated the decomposition of azidotetraphenylporphinatoiron(III) in the presence of bases and found the reaction to be extremely complicated. However, at high temperature, in the absence of added bases, the azide decomposition proceeded smoothly in pure xylene and provided an interesting product, $(TPPFe)_2N$, containing a nitrogen atom bridge analogous to the well-characterized μ-oxo dimer $(TPPFe)_2O$.[8-11] This appears to be the first example of a nitrogen bridged complex of a first transition series metal.

Experimental Section

All solvents and chemicals were reagent grade and used without further purification. Xylene was Fisher certified xylenes containing a mixture of ortho, meta, and para isomers which were dried and distilled from calcium hydride immediately prior to use.

Spectra were recorded on Perkin-Elmer Model 521 and Cary Model 14 spectrophotometers. Mass spectra were observed on a Hitachi Perkin-Elmer Model RMU-6E spectrometer. Mossbauer data were collected on a Ridl 400 channel analyzer, Model 34-12B, using an Elscint Mossbauer drive, Model MFD-4 in the sawtooth mode. Pulse height discrimination was performed with a high count rate amplifier (Elscint, Model CAV-N-1) and single channel analyzer (Elscint, Model SCA-N-2A). The data were analyzed by a conventional least-squares fit to individual Lorentzian shaped absorption peaks on an IBM 360-168 computer. The maximum error calculated for the position of any one absorption peak was ±0.002 mm/s. Low temperature spectra were obtained with an Air Products cryostat and a proportional temperature controller. Although the sample temperatures were held constant to within ±0.2 K the actual temperatures were known to only ±1.0 K. All spectra were observed using powders and isomer shifts are reported relative to iron metal.

Magnetic suceptibilities were measured on powdered samples by the Faraday method using an Ainsworth electronic balance and an Alpha cryostat between 77 and 300 K. $HgCo(SCN)_4$ was used as a standard and the magnetic field was measured using metallic nickel. Suceptibilities were corrected for diamagnetism using the value -386×10^{-6} cgs units/mol for tetraphenylporphine and the standard values for other elements present.[12]

Molecular weights were determined by vapor pressure osmometry on a Hitachi Model 115 unit in Fisher Spectrograde methylene chloride or benzene which was distilled from calcium hydride immediately prior to use. The system was calibrated with benzil and checked with μ-oxobis-(tetraphenylporphinatoiron(III)). This provided an estimate of the error in the observed molecular weight of ±5%.

***meso*-Tetraphenylporphine**, $C_{44}H_{30}N_4$ ($TPPH_2$), was prepared by the method of Adler et al.[13] or purchased from the Aldrich Chemical Co.

μ-Oxobis-(tetraphenylporphinatoiron(III)), [$(TPPFe)_2O$], was prepared by the method of Adler et al.[14] and purified by alumina chromatography with methylene chloride.

Tetraphenylporphinatoiron(III) Azide ($TPPFeN_3$). Hydrazoic acid was prepared from 150 ml of a saturated solution of NaN_3 on a Bio-Rad AG 50W-X8 cation exchange resin (wet volume 125 ml). The void volume was discarded. $(TPPFe)_2O$ (459 mg, 0.34 mmol) in 300 ml of freshly distilled benzene was shaken with 150 ml of the aqueous azide solution and the mixture was allowed to stand for 15 min. The aqueous layer was discarded and the benzene layer was washed three times with equal volumes of water. The benzene was removed under reduced pressure at 60 °C and the solid product was dried in vacuo over P_2O_5 for 24 h, yield 378 mg (78%).

Anal. Calcd for $C_{44}H_{28}N_7Fe$: C, 74.37; H, 3.97; N, 13.80; Fe, 7.86. Found: C, 74.64; H, 4.07; N, 13.91; Fe, 7.89.

Thermal Decomposition of $TPPFeN_3$ in Xylene. The hemin azide (826 mg, 1.16 mmol) was dissolved in 400 ml of freshly distilled xylene. The solution was refluxed under N_2 for 14 h and the solvent was removed in vacuo at 60 °C to quantitatively produce the product. The solid was washed with methanol and reprecipitated from CH_2Cl_2-petroleum ether. The purple powder was dried in vacuo over P_2O_5 for 48 h at 110 °C: yield 651 mg (83%); λ_{max} (xylene) 533 (ϵ 1.79×10^4 cm^2 mol^{-1}), 409 (ϵ 1.99×10^5), 380 nm (ϵ 1.80×10^5).

Anal. Calcd for $C_{88}H_{56}N_9Fe_2$: C, 78.23; H, 4.17; N, 9.33; Fe, 8.27. Found: C, 78.24, 78.13; H, 4.31, 4.30; N, 9.37, 9.31; Fe, 8.21, 8.30.

To identify the gas evolved during the reaction, analytically pure $TPPFeN_3$ was dissolved in xylene in a drying ampoule equipped with a breakseal and evacuated on a vacuum line. The ampoule was sealed with a torch while evaculated and the solution was heated to 138 °C for 14 h. The ampoule was attached to a mass spectrometer, the solution cooled in a liquid nitrogen bath, and the head gases introduced directly. The solution was examined by visible spectroscopy.

Conversion of $(TPPFe)_2N$ to $TPPH_2$. $(TPPFe)_2N$ (12.3 mg, 0.009 mmol) was dissolved in 50 ml of a 3:2 (v/v) $CHCl_3$-CH_3OH solution in a flask equipped with a reflux condenser. $FeCl_2 \cdot 6H_2O$ (250 mg, 1.1 mmol) was added to reduce the iron porphine. HCl was bubbled through the solution and the mixture was refluxed for 15 min upon which the solution became bright green. After cooling, the organic layer was washed twice with an equal volume of 3 M NaOH and the aqueous layer discarded. The organic solvent was removed in vacuo and the solid residue was identified as $TPPH_2$.

Kinetic Studies of the Formation of $(TPPFe)_2N$. Method A. A solution of $TPPFeN_3$ (1 mg/ml) in xylene (50 ml) was heated in a thermostated bath. The solution was stirred under a nitrogen atmosphere and aliquots were withdrawn via a serum cap. The reaction mixture was sampled for approximately one half-life, when the product began to precipitate. An infinity measurement was recorded after, 48 h. This was accomplished by transferring the remaining reaction mixture to a tared flask and weighing. A sufficient volume of xylene was added to dissolve all the product and the total solution weighed. All concentrations were determined by absorbance measurements.

Method B. A stock solution of $TPPFeN_3$ in xylene (1 mg/ml) was transferred in 4-ml aliquots into each of 12 5-ml drying ampoules. Each aliquot was then degassed and sealed under vacuum and the ampoules were then immersed in a thermostated bath. At the appropriate time a tube was removed from the bath and the reaction quenched immediately in liquid nitrogen. The tube was then opened, the contents transferred to a tared 25-ml flask, and the solution weighed. Fresh xylene was then added to bring the volume to 25 ml and the final weight recorded. The solution was stirred for several hours to dissolve the product and the absorbance measured.

Results

Decomposition of $TPPFe^{III}N_3$. Refluxing a xylene solution of $TPPFe^{III}N_3$ under nitrogen gas for 14 h produces a quantitative yield of a product found to be $(TPPFe)_2N$. In order to identify the gas produced during the reaction, the same conditions were employed for a solution in an evacuated tube. The identical porphine product was obtained and mass spectral analysis of the gas revealed that only N_2 was present. Substitution of xylene as the solvent by nitrobenzene at 140 °C or benzene at 120 °C produced a spectrally identical iron porphine product. The strong asymmetric stretch of the azide in $TPPFe^{III}N_3$ at 2055 cm^{-1} (KBr) disappears during the reaction and the product presents new infrared (KBr) absorptions at 910 cm^{-1} (vs, broad) and 885 cm^{-1} (m, sharp). Except for the 800–1000-cm^{-1} region shown in Figure 1, which includes the stretch of the μ-oxo bridge in $(TPPFe)_2O$, the infrared spectra of $(TPPFe)_2O$ and $(TPPFe)_2N$ are identical between 400 and 4000 cm^{-1}.

Further evidence that the porphine ring was not altered during the reaction was obtained by removal of the iron from the product to produce a material spectrally identical with authentic tetraphenylporphine.

If the formation of $(TPPFe)_2N$ is carried out in contact with the atmosphere, the product appears to be contaminated with $(TPPFe)_2O$. However, pure $(TPPFe)_2N$ itself is quite stable in air as a solid or in solution. A xylene solution of $(TPPFe)_2N$ showed no change in the visible spectrum after refluxing in air for several days. Formation of the product also depends on the concentration of $TPPFe^{III}N_3$. Even under nitrogen the reaction solution, after opening to air, will contain appreciable quantities of $(TPPFe)_2O$ if the initial concentration of $TPPFe^{III}N_3$ is less than 1 mg/ml.

Molecular weight measurements in CH_2Cl_2 or benzene substantiate a dinuclear formulation for the product (calcd for $(TPPFe)_2N$, 1351 g/mol) with 1356 g/mol being observed at a $(TPPFe)_2N$ concentration of 0.644 g/kg of CH_2Cl_2. However, some molecular association may be possible because as the $(TPPFe)_2N$ concentration was increased to saturation the observed molecular weight increased (e.g., 2230 g/mol at 2.10 g of $(TPPFe)_2N$/kg of CH_2Cl_2). The observed reaction is:

$$2TPPFeN_3 \rightarrow (TPPFe)_2N + \tfrac{5}{2}N_2$$

Magnetic Measurements. The magnetic properties of $TPPFe^{III}N_3$ are indicative of the expected high-spin d^5 system. $(TPPFe)_2N$ also exhibits simple paramagnetic behavior provided that the sample was prepared from a concentrated solution of $TPPFeN_3$ in xylene (2 mg/ml). At 86 K the susceptibility of the product is field independent from 600 to 6000 G. At a field of 6000 G the temperature dependence of the susceptibility presented in Table I follows Curie–Weiss behavior and a least-squares fit of the data indicates a magnetic moment of $\mu_{eff} = 2.04\ \mu_B$. The observed Weiss constant of +11° is within experimental error of zero. The analogous μ-oxo dimer $(TPPFe)_2O$ exhibits a moment which depends on temperature and upon the extent of prior drying of the sample. This behavior is not found for $(TPPFe)_2N$.

We have also observed that the preparation of $(TPPFe)_2N$ from solutions with an initial $TPPFeN_3$ concentration of less than 2 mg/ml sometimes generates a troublesome ferromagnetic impurity in the product. We have not been able to remove that impurity once it is present; however, even under these conditions the bulk material appears unchanged. That was revealed by a plot of $1/H$ vs. χ_g (at 80 K) for a sample of $(TPPFe)_2N$ which contained the unknown ferromagnetic impurity. Least-squares analysis of these data indicates that at infinite field

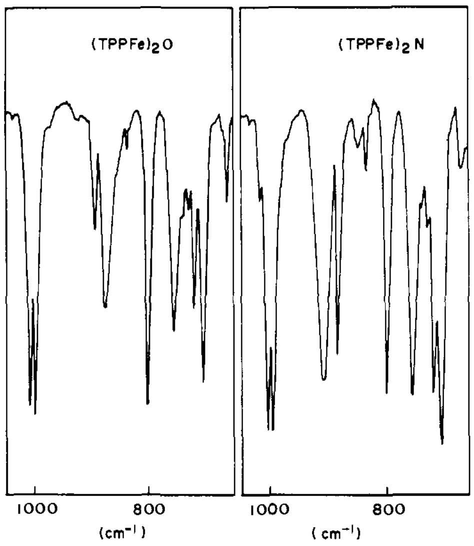

Figure 1. Partial infrared spectra of $(TPPFe)_2O$ and $(TPPFe)_2N$ in KBr.

Table I. Magnetic Susceptibility Data for $(TPPFe)_2N$

T, K	$10^6\chi_g$[a]	$10^6\chi_m$[b]	μ_{eff}[c]
86.5	3.49	5.51	1.96
101.1	2.88	4.69	1.96
125.8	2.46	4.12	2.04
147.8	1.74	3.13	1.93
174.2	1.42	2.72	1.95
198.1	1.22	2.45	1.98
222.4	1.01	2.17	1.97
248.2	0.891	2.00	2.00
296.8	0.696	1.74	2.04

[a] In cgs units/g. [b] In cgs units/mol, corrected. [c] Effective moment in Bohr magnetons per $(TPPFe)_2N$ unit.

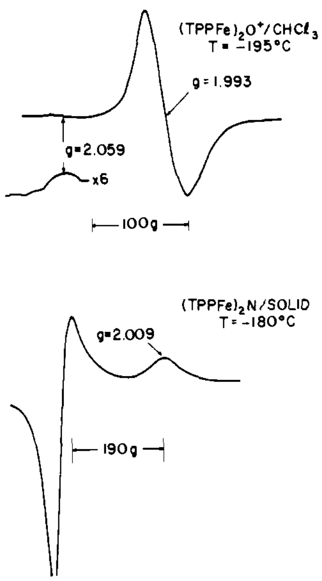

Figure 2. Electron paramagnetic resonance spectra observed for $[(TPPFe)_2O]^+$ [15] and $(TPPFe)_2N$.

Table II. Mossbauer Parameters

Compound	δ, mm/s[a]	Δ, mm/s[b]	Comments[c]
$(TPPFe)_2N$	0.099	1.08	300 K, $\Gamma = 0.35$
$(TPPFe)_2N$	0.148	1.07	77 K, $\Gamma = 0.44$
$(TPPFe)_2N$	0.173	1.08	44 K, $\Gamma = 0.46$
$(TPPFe)_2N$	0.170	1.08	24 K, $\Gamma = 0.45$
$(TPPFe)_2N$	0.166	1.08	6 K, $\Gamma = 0.48$
$TPPFe^{III}Im_2Cl$[d]	0.14	2.11	l.s., sharp at 300 K
$TPPFe^{III}py_2Cl$[d]	0.17	1.25	l.s., sharp at 77 K
$(TPPFe)_2O$[e]	0.29	0.62	h.s., sharp at 300 K
$TPPFe^{III}Cl$[f]	0.43	0.46	h.s., broad at 300 K
$TPPFe^{II}Im_2$[d]	0.46	1.06	l.s.. sharp at 77 K
$TPPFe^{II}py_2$[d,g]	0.38	1.20	l.s , sharp at 300 K

[a] Isomer shift relative to Fe metal. [b] Quadruple splitting. [c] Key: l.s. = low-spin, h.s. = high spin, Γ = full width at half-maximum absorption in mm/s. [d] Im = imidazole, L. M. Epstein, D. K. Straub, and C. Maricondi, *Inorg. Chem.*, **6**, 1720 (1967). [e] Reference 8. [f] Spectrum measured at 4.2 K, ref 16. [g] H. Kobayashi, Y. Maeda, and Y. Yanagawa, *Bull. Chem. Soc. Jpn.*, **43**, 2342 (1970).

the susceptibility of the sample is $\chi_m^c = 6730 \times 10^{-6}$ (cgs unit/mol) which corresponds to $\mu_{eff} = 2.04\ \mu_B$ per dimer.

While it is impossible to identify the impurity, a concentration of only 10 ppm of metallic iron would account for the magnitude of the observed field dendence of the susceptibility. The only effective way to avoid the presence of that impurity is by utilization of high concentrations (2 mg/ml) of $TPPFeN_3$ in the initial formation of $(TPPFe)_2N$.

The room temperature electron paramagnetic resonance spectrum of polycrystalline $(TPPFe)_2N$ shows only one broad (ca. 140 G) absorption at $g = 2.15$. Cooling the solid sample to below 193 K gradually produces a spectrum with the same $g = 2.15$ resonance and a new satellite at $g = 2.01$. No nitrogen hyperfine splitting has been observed in the spectra.

Figure 2 shows the observed spectrum and the EPR spectrum observed by Felton[15] for the $[(TPPFe)_2O]^+$ cation produced by electrochemical oxidation of $(TPPFe)_2O$. The temperature dependence of the satellite absorption is similar in the two spectra.

The NMR spectrum of $(TPPFe)_2N$ in $CDCl_3$ at room temperature was examined between 0 and 100 ppm (δ). Resonances were observed only at 7.1 and 8.3 ppm similar to that observed for $(TPPFe)_2O$ and $[(TPPFe)_2O]^+$.

Mossbauer Spectra. The Mossbauer spectra of high-spin d^5 iron porphyrins such at $TPPFe^{III}N_3$ show dramatic broadening at temperatures above 5 K due to spin-relaxation effects at the isolated iron(III) centers.[16,17] Such broadening is not observed in the spectrum of $(TPPFe)_2O$ due to the antiferromagnetic interactions between the two high-spin iron atoms.[8,10,11] Low spin iron(II) or -(III) porphyrins generally also present sharp room temperature Mossbauer spectra.

The Mossbauer spectrum observed for polycrystalline $(TPPFe)_2N$ is sharp and symmetrical at all temperatures utilized between 300 and 6 K. The spectra observed at the two temperature extremes are shown in Figure 3. Although the line widths and intensities of the spectral peaks changed with temperature, the line widths, intensities, and areas of the positive velocity peaks were within experimental error always equal to those of the negative velocity peaks. The data are compared to that for some related compounds in Table II.

Kinetic Studies. Rate studies of the thermal conversion of $TPPFe^{III}N_3$ to $(TPPFe)_2N$ are complicated by two experimental facts: (A) using a low initial concentration of $TPPFe^{III}N_3$ and temperatures below 125 °C, the product is not pure but contains some $(TPPFe)_2O$; (B) using high initial concentrations of $TPPFe^{III}N_3$ causes precipitation of the product before one half-life and because of spectral overlap of the reactant and product the observed optical density of the solution is difficult to interpret. This problem was avoided by using two different methods to follow the course of the reaction. At temperatures above 125 °C, reaction mixtures containing varying initial concentrations were

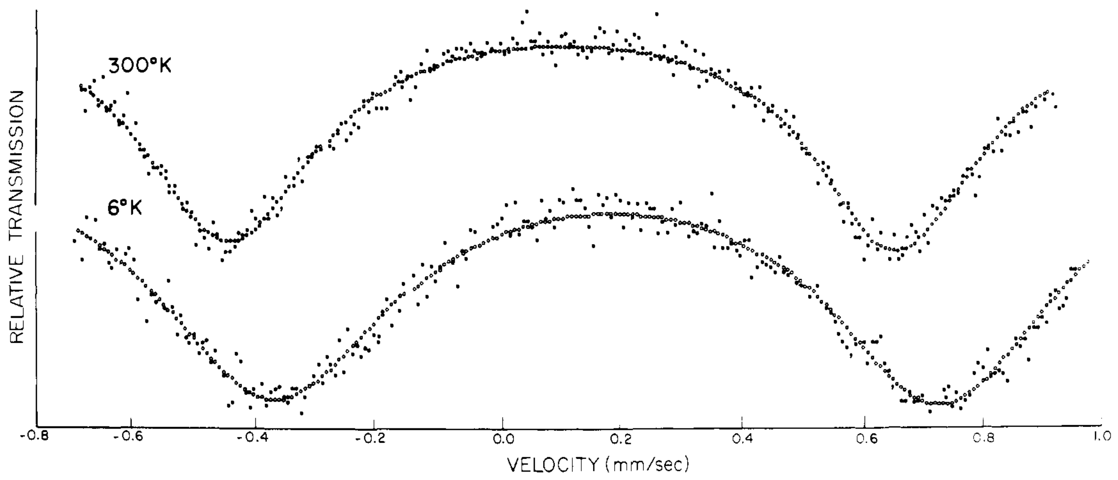

Figure 3. Mossbauer spectra of $(TPPFe)_2N$ at 6 and 300 K relative to iron metal. Open circles represent the least-squares fitted curve and closed circles represent only those data points which do not fall on the calculated curve. All other data points fall on the calculated curve.

Table III. Kinetic Data for the First-Order Decomposition of $TPPFe^{III}N_3$ in Xylene

T, °C	Method[a]	10^4k, s^{-1}
115	B	0.58
120	B	1.16
125	A	1.86
126	A	2.27
126	A	2.36
126	A	2.24
130	B	2.89
130	A	3.04

[a] Key: A = under N_2 atmosphere, B = in vacuo, see text for details.

Table IV. Frequencies of the Asymmetric Stretch for M-X-M Systems

System	ν, cm^{-1}
$(TPPFe)_2N$	910 (vs), 885 (m)
$(TPPFe)_2O$[a]	885 (m), 870 (vs)
M_2X, X = N[b]	1000-1160
X = O[c]	700-900
M_2XH, X = N[d]	ca. 660
X = O[d]	500-580
M_2XH_2, X = N[d]	ca. 540

[a] Reference 8. [b] M equals only second or third transition series metals, W. P. Griffith, *Coord. Chem. Rev.*, **8**, 369 (1972). [c] W. P. Griffith, *Coord. Chem. Rev.*, **5**, 459 (1970). [d] D. J. Hewkin and W. P. Griffith, *J. Chem. Soc. A*, 472 (1966), and references therein.

followed for one half-life by spectrophotometric assay of the homogeneous solutions under a static head of nitrogen gas. Triplicate determinations of the reaction rate at 126 °C gave rate constants that varied by ±2.5%. At temperatures below 125 °C the reactions were run in sealed evacuated ampoules, and the product was allowed to precipitate. At specific intervals up to four half-lives the ampoules were opened and the heterogeneous solutions were diluted sufficiently to dissolve all solids. The resultant solutions were assayed spectrophotometrically. Both methods were used at 130 °C and the observed rate constants differed by 5%.

All reaction runs were observed to closely follow first-order kinetics in $TPPFe^{III}N_3$ for as long as they were followed but not more than 3.5 half-lives. They showed large scatter beyond four half-lives. The data are summarized in Table III. The activation energy was observed to be 33.7 kcal/mol.

Discussion

The slow thermal decomposition of $TPPFe^{III}N_3$ quantitatively produces $(TPPFe)_2N$. The formulation of the product is substantiated by elemental analysis, molecular weight measurements, proven integrity of the porphine ring, and observation of reasonable NMR, visible, and infrared spectra. The product is considered similar to, but not isoelectronic with, $(TPPFe)_2O$. A nitrogen bridged dimer isoelectronic with $(TPPFe)_2O$ would be, for example, $(TPPFe)_2NH$. However, the presence of an NH (or for that matter NH_2) bridge can be eliminated by consideration of the infrared data summarized in Table IV. The infrared absorptions involving the nitrogen bridge in the product are 200-300 cm^{-1} above the region characteristic of known dinuclear M_2NH (and M_2NH_2) species and fall close to the region known for the M_2N stretch.

Most convincingly, any compound isoelectronic with $(TPPFe)_2O$ must be an even electron system and the product is clearly a paramagnetic doublet.

Because of the known hydrogen donor ability of xylene, the decomposition of $TPPFeN_3$ was also carried out in the poor hydrogen donor solvents benzene and nitrobenzene with no change in the product or its quantitative formation.

The infrared spectra of dinuclear oxygen and nitrogen bridged species have been well studied and frequencies of the asymmetric MXM stretch are presented in Table IV for several types of compounds. The difference between the known μ-nitrido and μ-oxo compounds can be rationalized in terms of the stronger π-donating properties of the nitride due to both the lower electronegativity and higher negative charge of N^{3-} as opposed to O^{2-}. It is also interesting to note that nitride bridged compounds have only been reported for metals of the second and third transition series which may also account for a great degree of π-bonding between the metals and the bridge atom. The fact that the data in Table IV for known M_2N derivatives only includes compounds where M is a second or third transition series element also explains the lower frequency of the Fe_2N asymmetric stretch observed for $(TPPFe)_2N$. In addition to decreased π-bonding due to the nature of the metal the data may also indicate the nitrogen bridge in $(TPPFe)_2N$ does not carry as great a negative charge as the nitride bridges included in the table. It would be useful to compare $(TPPFe)_2N$ with authentic nitride bridged compounds of the first transition series to fully evaluate the infrared data, but those compounds are not yet available. Comparison of the infrared spectra of $(TPPFe)_2O$ and $(TPPFe)_2N$ is consistent with a greater degree of bonding in the Fe_2N bridge.

Magnetic susceptibility measurements between 80 and

300 K indicate that $(TPPFe)_2N$ is a simple paramagnet. The moment, $\mu_{eff} = 2.04\ \mu_B$ per $(TPPFe)_2N$ molecule, is reasonable for one unpaired electron and the temperature independence of the moment eliminates an antiferromagnetic system with a thermally accessible high spin state as is found for $(TPPFe)_2O$.

Extensive molecular orbital calculations have been carried out for μ-oxo bridged dinuclear ions.[18] The orbital sequence depends on the linearity of the MOM bridge and on the extent of π-bonding in the bridge. Figure 4 shows the orbital ordering for a linear and bent bridge and adequately describes the temperature dependent moment of $(TPPFe)_2O$ which possesses a slightly bent FeOFe bridge (174.5°) and 18 electrons. The same scheme predicts that a 17-electron system possessing either a linear or slightly bent bridge should behave as a temperature independent doublet as is found for $(TPPFe)_2N$.

The μ-oxo dimer $(TPPFe)_2O$ has also been described[19] as two antiferromagnetically coupled $S = 5/2$ ions with a $J = 309\ \text{cm}^{-1}$. The $(TPPFe)_2N$ system can of course be described similarly but with a much larger value of J and the temperature independence of the moment precludes the assignment of the spin states of the individual iron atoms.

The hematin cation, $[(TPPFe)_2O]^+$, studied by Felton,[15] has a temperature dependent magnetic moment similar to its parent. The orbital vacancy has been assigned to the Fe_2O system, as opposed to a π-cation radical localized on the porphine ring, on the basis of NMR studies. According to Felton a π-cation radical formalism would require NMR shifts of 20–40 ppm, which were not observed for $[(TPPFe)_2O]^+$. The smaller chemical shifts also found in the NMR spectrum of $(TPPFe)_2N$ thus supports the electron configuration presented above. The similarity of the temperature dependence of the ESR spectra found for $(TPPFe)_2N$ and $[(TPPFe)_2O]^+$ may be due to their isoelectronic relationship.

The Mossbauer spectrum of $(TPPFe)_2N$ presents a temperature independent doublet indicating that the two iron atoms are either in the same oxidation state and environment or the occurrence of very rapid ($<10^{-7}$ s) exchange between the two. The Mossbauer parameters can thus provide some insight to the average, or static, state of the iron atoms.

The data in Table II indicate that for the TPPFe series the isomer shifts of high spin Fe(III) compounds are higher than those of the low-spin series in accord with a greater amount of metal to ligand π-bonding from the lower spin state ion. The large difference in quadruple splitting indicates that electronic effects are more important than site symmetries in determining the electronic field gradients for the two spin states of iron(III). Thus $(TPPFe)_2O$ presents Mossbauer spectral parameters indicative of antiferromagnetically coupled high spin iron(III) ions in agreement with other evidence. Considering the transition from $(TPPFe)_2O$ to $(TPPFe)_2N$, the decrease in isomer shift and the increase in quadruple splitting could be taken to indicate a change of spin state with $(TPPFe)_2N$ possessing low spin Fe(III) ions. However, all solid low spin $TPPFe^{III}$ systems are six coordinate and all solid five-coordinate $TPPFe^{III}$ compounds are high spin. $TPPFe^{III}CN$ has recently been reported to be low spin in Me_2SO solution, but no solids have been isolated and the complex may contain Me_2SO as a sixth ligand.[20] Because solid $(TPPFe)_2N$ contains two five-coordinate iron atoms, a low spin configuration would be unusual.

Consideration of the differing electronic configurations of the Fe_2O and Fe_2N systems described above leads to a reasonable interpretation of the Mossbauer parameters of both binuclear compounds as coupled high-spin ions. The orbital vacancy in $(TPPFe)_2N$ (compared to $(TPPFe)_2O$) is in an antibonding π-orbital involving the Fe d orbitals. If that orbital is (as is reasonable) appreciably metallic in character, the two iron atoms in $(TPPFe)_2N$ possess up to one d electron less than for $(TPPFe)_2O$. Removal of up to half a d electron from each iron atom would lead to a decrease in isomer shift, as is observed. At the same time the two high spin iron atoms in $(TPPFe)_2O$ have a symmetrical electronic configuration and low quadruple splitting. Removal of d electron density from the π-system would decrease that symmetry and cause an increase in quadruple splitting, as is observed. Thus the Mossbauer parameters are consistent with a formalism of $(TPPFe)_2N$ where both iron atoms have an oxidation state higher than three and may be presented as a N(−III) bridge between two Fe(+III½) ions. There are of course many other possible formalisms involving other oxidation states of the bridge atom or differing oxidation states of the two iron atoms and rapid valence exchange between them. Our observation of broadening of the Mossbauer spectrum at liquid He temperatures may indicate that such is the case but on the time scale (10^{-7} s) of the Mossbauer experiment, the two iron atoms are equivalent at temperatures above the liquid He region.

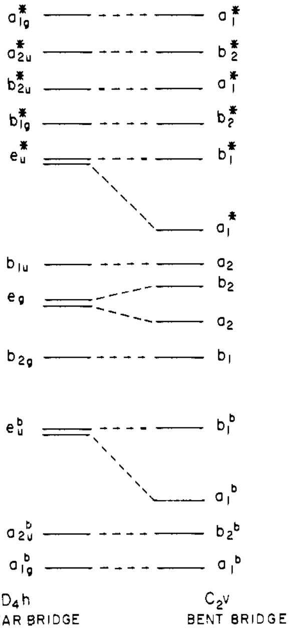

Figure 4. Molecular orbital schemes for the M-X-M system in linear and bent conformations.[18] The highest populated orbital in the linear extreme is the π^* orbital $(TPPFe)_2O$, $(e_u^*)^2$; $(TPPFe)_2N$, $(e_u^*)^1$.

The kinetically clean first-order decomposition of $TPPFeN_3$ is consistent with any mechanism including reaction 1 as the rate determining step.

$$TPPFeN_3 \rightarrow [TPPFeN] + N_2 \qquad (1)$$

There are at least two reasonable schemes which can be presented for the product formation after the rate determining step.

Scheme I

$$[TPPFeN] + TPPFeN_3 \rightarrow (TPPFe)_2N + N\cdot_3 \qquad (2)$$

$$2N\cdot_3 \rightarrow 3N_2 \qquad (3)$$

Scheme II

$$[TPPFeN] + TPPFeN_3 \rightarrow [(TPPFe)_2N_4] \qquad (4)$$

$$[(TPPFe)_2N_4] \rightarrow 2[TPPFeN_2] \qquad (5)$$

$$[TPPFeN_2] \rightarrow TPPFe + N_2 \qquad (6)$$

$$[TPPFeN] + TPPFe \rightarrow (TPPFe)_2N \qquad (7)$$

The two schemes differ in the behavior of TPPFeN. In step 2, TPPFeN attacks $TPPFeN_3$ at the open coordination site of the metal and could be considered a nucleophilic pathway. In step 4, TPPFeN attacks $TPPFeN_3$ at the azide and is thus an electrophilic pathway. Step 5 produces $TPPFe^{II}N_2$, which is still unknown and thus proposed to lose N_2. The $TPPFe^{II}$ formed is attacked at the metal by TPPFeN to produce the product in step 7.

The evaluation of the reaction scheme after step 1 will thus provide insight into the nucleophilicity of the intermediate TPPFeN. This will then allow the assignment of TPPFeN as either a nitrene or a nitride species. Further experiments are in progress regarding this question.

Finally, the difference in the degree of magnetic coupling between the two iron atoms in $(TPPFe)_2N$ and $(TPPFe)_2O$ is striking. It is not obvious to us why the N bridge should be so effective in this regard although there are no other N-bridged first transition series dinuclear metal complexes with which a comparison can be drawn.

Acknowledgment. This work was supported by the National Institutes of Health through Grant No. AM 17331.

References and Notes

(1) (a) Portions of this work were presented at the 169th National Meeting of the American Chemical Society, Philadelphia, Pa., April 1975, Abstracts, paper INOR 7. (b) Taken from the dissertation of D. A. Summerville, submitted to the Faculty of the Polytechnic Institute of New York in partial fulfillment of the requirements for the degree of Doctor of Philosophy in Chemistry, 1975.
(2) Brooklyn College.
(3) A. D. Allen, R. O. Harris, B. R. Loescher, J. R. Stevens, and R. N. Whiteley, *Chem. Rev.*, **73**, 11 (1973).
(4) L. A. P. Kane-Maguire, P. S. Sheridan, F. Basolo, and R. G. Pearson, *J. Am. Chem. Soc.*, **92**, 5865 (1970).
(5) B. C. Lane, J. W. McDonald, F. Basolo, and R. G. Pearson, *J. Am. Chem. Soc.*, **94**, 3786 (1972).
(6) P. S. Sheridan and F. Basolo, *Inorg. Chem.*, 11, 2721 (1972).
(7) W. S. Caughey and S. McCoy, *Biochemistry*, **9**, 2387 (1970).
(8) I. A. Cohen, *J. Am. Chem. Soc.*, **91**, 1980 (1969).
(9) A. B. Hoffman, D. M. Collins, V. W. Day, E. B. Fleischer, T. S. Srivastava, and J. L. Hoard, *J. Am. Chem. Soc.*, **94**, 3620 (1972).
(10) G. N. LaMar, G. R. Eaton, R. H. Holm, and F. A. Walker, *J. Am. Chem. Soc.*, **95**, 63 (1973).
(11) M. A. Torrens, D. K. Straub, and L. M. Epstein, *J. Am. Chem. Soc.*, **94**, 4160 (1972).
(12) B. H. Figgis and T. Lewis in "Modern Coordination Chemistry", T. Lewis and R. G. Wilkins, Ed., Interscience, New York, N.Y., 1960, p 403.
(13) A. D. Adler, F. R. Longo, T. D. Finarelli, T. Goldmacher, T. Assour, and L. Korsakoff, *J. Org. Chem.*, **32**, 476 (1967).
(14) A. D. Adler, F. R. Longo, F. Kampas, and T. Kim, *J. Inorg. Nucl. Chem.*, **32**, 2443 (1970).
(15) (a) R. H. Felton, G. S. Owen, D. Dolphin, and T. Fajer, *J. Am. Chem. Soc.*, **93**, 6332 (1971); (b) R. H. Felton, G. S. Owen, D. Dolphin, A. Forman, D. C. Borg, and T. Fajer, *Ann. N.Y. Acad. Sci.*, **206**, 504 (1973).
(16) C. Maricondi, D. K. Straub, and L. M. Epstein, *J. Am. Chem. Soc.*, **94**, 4157 (1972).
(17) M. Blume, *Phys. Rev. Lett.*, **18**, 305 (1967).
(18) B. Jezowska-Trzebiatowska, *Pure Appl. Chem.*, **27**, 89 (1971).
(19) P. D. W. Boyd, and T. D. Smith, *Inorg. Chem.*, **10**, 2041 (1971).
(20) J. T. Wang, H. J. C. Yeh, and D. F. Johnson, *J. Am. Chem. Soc.*, **97**, 1968 (1975).

The Synthesis, Structures, and Properties of New Macrocyclic Ligands and Novel Sexadentate Iron Complexes Produced by Electrophilic Reactions of the Iron Derivatives

Dennis P. Riley,[1a] John A. Stone,[1b] and Daryle H. Busch*[1a]

Contribution from The Evans Chemical Laboratory, The Ohio State University, Columbus, Ohio 43210, and the Savannah River Laboratory, E. I. duPont de Nemours and Co., Aiken, South Carolina 29801. *Received July 28, 1975*

Abstract: A template synthesis of ionizable 14-, 15-, and 16-membered tetraaza, tetraene macrocyclic ligands, devoid of functional substituents, has been devised. Also, the synthesis of six-coordinate dicationic iron(II) complexes of the new ligands are described. For the 14-membered ligand a trans diacetonitrile complex was obtained, but for both the 15- and 16-membered ligands, acetonitrile molecules add electrophilically to the γ-carbons of the macrocycle, producing the complex of novel sexadentate ligands. The latter represent examples in which coordinate saturation is achieved by the appending of two donor groups to a tetradentate macrocyclic ligand. These structures are formally analogous to such natural heme proteins as cytochrome *c*.

In recent years many advances have been made in the design and synthesis of tetraaza macrocyclic ligands and their transition metal complexes.[2-5] Systematic variations in ring size, unsaturation, and substituents have provided a basis for elucidating and understanding the effects these structural features have on both physical and chemical properties.[5-7] The subject of this study has been the preparation of new 14-, 15-, and 16-membered tetraaza, tetraene macrocyclic ligands, devoid of functional substituents, and the synthesis and characterization of their novel complexes with the biologically significant metal iron.

The ligands II have been prepared via a template route based on the work of Jager[8,9] and the observation of Hipp and Busch[10] that the 15-membered Jager complex (Ib) can be deacylated by strong acid in a nucleophilic solvent. In addition, a 16-membered ligand, structurally analogous to the ligands II, was synthesized by a modification of the procedure used by Holm and co-workers[4] for preparation of ligand IIIa.

The synthesis of the iron(II) complexes of these new ligands has led to the isolation and characterization of a series of low-spin six-coordinate dicationic complexes. For the 14-membered ligand a *trans*-diacetonitrile, "bis-β-diimine" complex (structure IV) was obtained, but for the 15- and 16-membered ligands, complexes were obtained which displayed physical and chemical properties totally unlike those exhibited by the 14-membered complex. In order to determine the correct structure of these latter complexes, a de-